Phase Composition and Photocatalytic Activity of TiO_2-Fe_3O_4 Coatings Prepared by Plasma Spraying Technique†

YE Fuxing* and OHMORI Akira**

Abstract

Owing to the much concern with global environmental problem, photocatalytic TiO_2 coatings were obtained using plasma spraying technique. The influence of the content of Fe_3O_4 additive to the TiO_2 powder on the phase composition, microstructure and photo-absorption of plasma sprayed TiO_2 coatings was systematically studied. The photocatalytic efficiency of the sprayed coatings was evaluated through the photo degradation of acetaldehyde. The UV-VIS-NIR absorption spectra of the deposited coatings were obtained by using Shimadzu UV-3100PC scanning spectrophotometer. The results showed that the TiO_2-Fe_3O_4 coatings consist of anatase TiO_2, rutile TiO_2, and Fe_2TiO_5 pseudobrookite phase which appears when the content of Fe_3O_4 additive is equal to or over 10%. The content of $FeTiO_3$ is highest in the sprayed TiO_2-10%Fe_3O_4 coatings. The content of anatase TiO_2 in the sprayed coatings decreases with the increasing of Fe_3O_4 content. The addition of Fe_3O_4 decreases the anatase-rutile transformation temperature according to the heat treatment results of feedstock powders. It was found that TiO_2 coatings can decompose acetaldehyde under the illumination of ultraviolet rays, and the degrading efficiency is improved with an increase in the content of $FeTiO_3$ in the coatings. However, presence of large amount of Fe_2TiO_5 compound substantially lowers the photocatalytic efficiency of the sprayed TiO_2-Fe_3O_4 coatings for its unfavorable photo-excited electron-hole transfer process.

KEY WORDS: (Photocatalytic) (Plasma spraying) (TiO_2) (Fe_3O_4) (Photo absorbance)

1. Introduction

In the 1980's, the UN set up the World Commission on Environment and Development, also called the Brundtland Commission. They produced *"Our Common Future"*, otherwise known as the Brundtland Report. It defined sustainable development as development which;

"meets the needs of present generations without compromising the ability of future generations to meet their own needs"

To solve the environmental problems related to the hazardous wastes, contaminated groundwater and toxic air contaminants, extensive research is underway to develop commercial photocatalysts, which involve in TiO_2, CdS, SnO_2, WO_3, SiO_2, ZrO_2, ZnO, Nb_2O_5, Fe_2O_3, $SrTiO_3$ etc.[1)-11)]. Among all the oxide semiconductors that have been reported, titanium dioxide is an excellent photocatalyst due to its optical and electronic properties, chemical stability, non-toxicity and low cost[12)-17)]. However, it has been also realized that the forbidden energy gap of anatase TiO_2 (about 3.2eV) means that the electron can only be excited from the valence to the conduction band by the high power UV light irradiation with a wavelength less than 387nm. This limits the application of sunlight as an energy source for the photocatalysis. Recently, there have many methods to improve photocatalytic activity of the TiO_2 by ion implantation and adding the other semiconductor such as WO_3, Al_2O_3, Fe_3O_4 etc.[6)-11)].

The plasma spraying technique is widely used to deposit coating. In this study, the TiO_2 and TiO_2-Fe_3O_4 coatings were deposited on stainless steel (JIS SUS304) by plasma spraying technique, and effects of Fe_3O_4 content in the TiO_2-Fe_3O_4 feedstock powders on the phase composition and photocatalytic activity of the TiO_2 coatings were analyzed with scanning electron microscopy (SEM), energy dispersive analysis of X-ray (EDAX), X-ray diffraction (XRD), UV-3100PC scanning spectrophotometer and photocatalytic efficiency evaluation system in detail.

2. Materials and experimental procedures

2.1. Feedstock powders and substrate

It was found that the addition of Fe_3O_4 could enhance the photocatalytic efficiency of TiO_2 coatings[11)], but the influence of Fe_3O_4 content is still unclear. To

† Received on May 30, 2003
* Graduate Student, Osaka University
** Professor

Transactions of JWRI is published by Joining and Welding Research Institute of Osaka University, Ibaraki, Osaka 567-0047, Japan

study the effects of Fe_3O_4 particles on the photocatalytic activity of TiO_2-Fe_3O_4 coatings in detail, five kinds of composite powders were designed, these were TiO_2-5wt.%Fe_3O_4, TiO_2-10wt.%Fe_3O_4, TiO_2-12.7wt.% Fe_3O_4, TiO_2-22.5wt.%Fe_3O_4 and TiO_2-32.6wt.%Fe_3O_4 powders. The average sizes of TiO_2 and TiO_2-Fe_3O_4 powders were about 32μm. The morphology of TiO_2 powder was spherical shape, which was very similar with TiO_2-Fe_3O_4 powders. It is very clear that the Fe_3O_4 additive was distributed uniformly in the agglomerated powder according to the EDAX maps. The substrate was stainless steel (JIS SUS304)

2.2 Coatings preparation and heat treatment of feedstock powders

The thermal spraying equipment was a plasma spraying system (Plasmadyne-Mach1 manufactured by Plasmadyne Company). Argon was used as a primary plasma gas and helium was used as the secondary gas. The thermal spraying parameters are given in **Table 1.** Except the specimen preparation to study phase changes of TiO_2-32.6%Fe_3O_4 coating after crush and heat treatment, which arc current of 600A was chosen, arc current of 400A was applied.

The anatase-rutile transformation temperature of pure anatase TiO_2 powder was approximate to 1173K. To investigate the influence of the additive on the anatase-rutile phase transformation temperature and compare the composition variations of feedstock powders in heat treatment process and in thermal spray process, they were kept in electric furnace for 7200s after reaching at treated temperature (973K, 1123K, 1273K or 1423K) with a heating rate of 0.167K/s, and then were cooled with the furnace.

Table 1 Plasma spraying parameters

Ar gas pressure (MPa) /flow (slpm)	0.42/58
He gas pressure (MPa) /flow (slpm)	0.21/9
Arc current (A)	400, 600
Arc voltage (V)	28~30
Spraying distance (mm)	70

2.3 Analysis of the feedstock powders and sprayed Coatings

Scanning electron microscope (SEM) and energy dispersive analysis of X-ray (EDAX) were used to examine the structure characteristics of the feedstock powders and the sprayed coatings. The phase composition of the heat treated powders and the sprayed coatings was investigated by X-ray diffraction using Cu-Kα radiation (λ=1.5406Å) and graphite crystal monochromator (JDX3530, JEOL, Japan). The 2θ range was 23°~38° including the main diffraction line of the possible phase compositions. Quantitative analysis of the phase composition of the heat treated powders was attempted by comparing the integrated X-ray diffraction peaks for anatase (101), rutile (110), Fe_2O_3 (104), $FeTiO_3$ (104) and Fe_2TiO_5 (101) phase. The weight contents of anatase TiO_2, rutile TiO_2, Fe_2O_3, $FeTiO_3$ and Fe_2TiO_5 compound were calculated by equations (1)~(6), respectively. The peak intensity relations have been established experimentally from powders mixture to known compositions to serve as standards, and the validity of this method was confirmed. However, it is extremely complex to consider the sprayed coatings applying equations (1)~(6) because preferred orientation and amorphous phase exist widely in thermal sprayed coating[18)-20)].

$$\frac{W_{Anatase}}{W_{Rutile}} = C_1 \frac{I_{Anatase(101)}}{I_{Rutile(110)}} \quad (1)$$

$$\frac{W_{Fe_2O_3}}{W_{Rutile}} = C_2 \frac{I_{Fe_2O_3(104)}}{I_{Rutile(110)}} \quad (2)$$

$$\frac{W_{FeTiO_3}}{W_{Rutile}} = C_3 \frac{I_{FeTiO_3(104)}}{I_{Rutile(110)}} \quad (3)$$

$$\frac{W_{Fe_2TiO_5}}{W_{Rutile}} = C_4 \frac{I_{Fe_2TiO_5(101)}}{I_{Rutile(110)}} \quad (4)$$

$$W_{Anatase} + W_{rutile} + W_{Fe_2O_3} + W_{FeTiO_3} + W_{Fe_2TiO_5} = 1 \quad (5)$$

$$W_{AnataseToRutile} = \frac{W_{rutile}}{W_{anatase} + W_{Rutile}} \quad (6)$$

where $I_{Anatase(101)}$ is the integrated intensity of the (101) reflection of anatase phase, $I_{Rutile(110)}$ the integrated intensity of (110) reflection of rutile phase, $I_{Fe2O3(104)}$ the integrated intensity of the (104) reflection of Fe_2O_3, $I_{FeTiO3(104)}$ the integrated intensity of (104) reflection of $FeTiO_3$ phase, $I_{Fe2TiO5(101)}$ the integrated intensity of (101) reflection of Fe_2TiO_5 phase, $W_{Anatase}$, W_{Rutile}, W_{Fe2O3}, W_{FeTiO3} and $W_{Fe2TiO5}$ the weight fractions of anatase TiO_2, rutile TiO_2, Fe_2O_3, $FeTiO_3$ and Fe_2TiO_5, respectively, and C_1, C_2, C_3 and C_4 the constants which are dependent on the crystal structures and lattice parameters of the upper mentioned substances. $W_{AnataseToRutile}$ the weight fraction of rutile transformed from anatase phase.

2.4 Diffuse reflectance spectroscopy and calculation of energy absorbance

The UV-VIS-NIR spectra of the feedstock powders and plasma sprayed coatings were recorded using a Shimadzu UV-3100PC scanning spectrophotometer

equipped with a diffuse reflectance accessory. The absorption intensity was calculated from the Kubelka-Munk equation as $f(R)=(1-R)^2/2R$, where $f(R)$ is Kubelka-Munk value and R is diffuse reflection of the coating. The integrated energy absorbance from the light source of the sprayed coatings was estimated according to the following equation.

$$E_{total} = \int E(\lambda) f(R_\lambda) d\lambda \qquad (7)$$

where $E(\lambda)$ is spectral irradiance of the light source, $f(R_\lambda)$ Kubelka-Munk value and E_{total} relative integrated energy absorbance. Generally, the increasing of E_{total} benefits to increase the photocatalytic activity[21].

The study of the tail of the absorption curve of semiconductor shows that it has a simple exponential increase. The onset of this increase (point A in **Fig.1**) has been suggested as a universal method of deducing the position of the absorption edge[22), 23)]. In this study, the wavelength coordinate of the point on the low wavelength side of the curve at which the liner increase in absorbance starts was marked to investigate the absorption shift of feedstock powders and sprayed coatings.

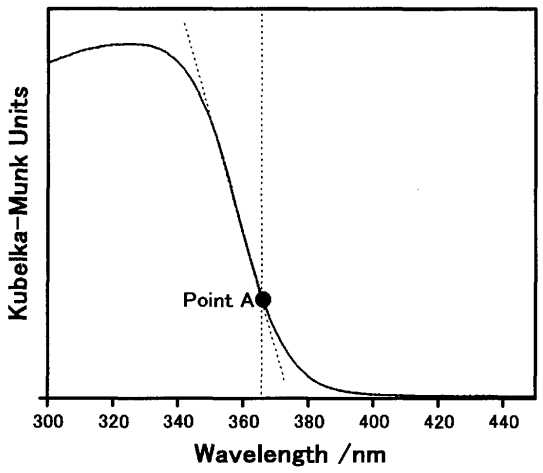

Fig.1 Definition of absorption edge in absorption spectrum of semiconductor.

2.4 Evaluation method of photocatalytic activity

In this experiment, the photocatalytic activity of the sprayed coatings was evaluated through the photo mineralization of acetaldehyde. The ultraviolet light (peak wavelength was 352nm) intensity on the sample surface was set in $1.0mW/cm^2$. In the experimental procedure, the decomposition of the concentration (ppm) of the foul gas with time (s) was measured with a Kitakawa type gas detector at a certain time interval.

The results for photocatalytic efficiency of titanium dioxide indicated that the destruction rates of various contaminants by photocatalyst fit the Langmuir-Hinshelwood kinetic equation[24), 25)]. The Langmuir-Hinshelwood rate form is

$$\ln(\frac{C_0}{C}) = t/\tau \qquad (8)$$

where C is the concentration of the reactant (ppm), C_0 the initial concentration of the reactant (ppm), t the irradiation time (s), τ the constant of photocatalytic activity. According to equation (8), the smaller of the τ value the better of the photocatalytic activity of the coatings.

3. Results and Discussion

3.1 Heat treated TiO_2 and composite TiO_2-Fe_3O_4 powders

Fig. 2 shows the x-ray diffraction results of TiO_2 and TiO_2-Fe_3O_4 feedstock powders heat treated at various temperatures. At 973K, anatase TiO_2 kept its crystal structure, but magnetite (Fe_3O_4) additive disappeared and Fe_2O_3 formed consequently (Fig.2(A)). At 1123K, one part of anatase TiO_2 transformed into rutile in composite powders, which did not take place for pure anatase TiO_2 powder. The content of anatase TiO_2 in heat treated powders, which was calculated according to equations (1)~(6), decreased with the increasing of Fe_3O_4 amount as shown in **Fig.3(a)**. The weight fractions of anatase transformed to rutile increases gradually (**Fig.3(b)**). These implied that the addition of Fe_3O_4 improve the anatase-rutile transformation.

Under more increased temperature at 1273K, anatase phase transformed completely to rutile in composite TiO_2-Fe_3O_4 powders. Under the higher temperature at 1423K, all Fe_2O_3 reacted with TiO_2 and produced stable Fe_2TiO_5.

3.2 Compositions of plasma sprayed TiO_2 and TiO_2-Fe_3O_4 coatings

The x-ray diffraction patterns of plasma sprayed TiO_2 and TiO_2-Fe_3O_4 coatings are illustrated in **Fig.4**. The relative intensity of anatase phase decreased with the increasing of Fe_3O_4 amount, which implied that the feedstock powders were more melted with the addition of Fe_3O_4. This was in good agreement with the results of heat treated feedstock powders discussed in section 3.1. Ilmenite $FeTiO_3$ phase appeared with the addition of Fe_3O_4 till 12.7%, but became undetectable with the amount over 22.5%. The relative intensity of $FeTiO_3$ was highest in TiO_2-10%Fe_3O_4 coating comparing with other coatings, which indicated that this coating had the highest content of $FeTiO_3$ compound. However, $FeTiO_3$ phase did not appear in heat treated powders. The peak intensity of Fe_2TiO_5 phase increased continuously and significantly with the increasing of Fe_3O_4 amount, and finally became the main phase with the almost complete disappearance of $FeTiO_3$ in the sprayed coating.

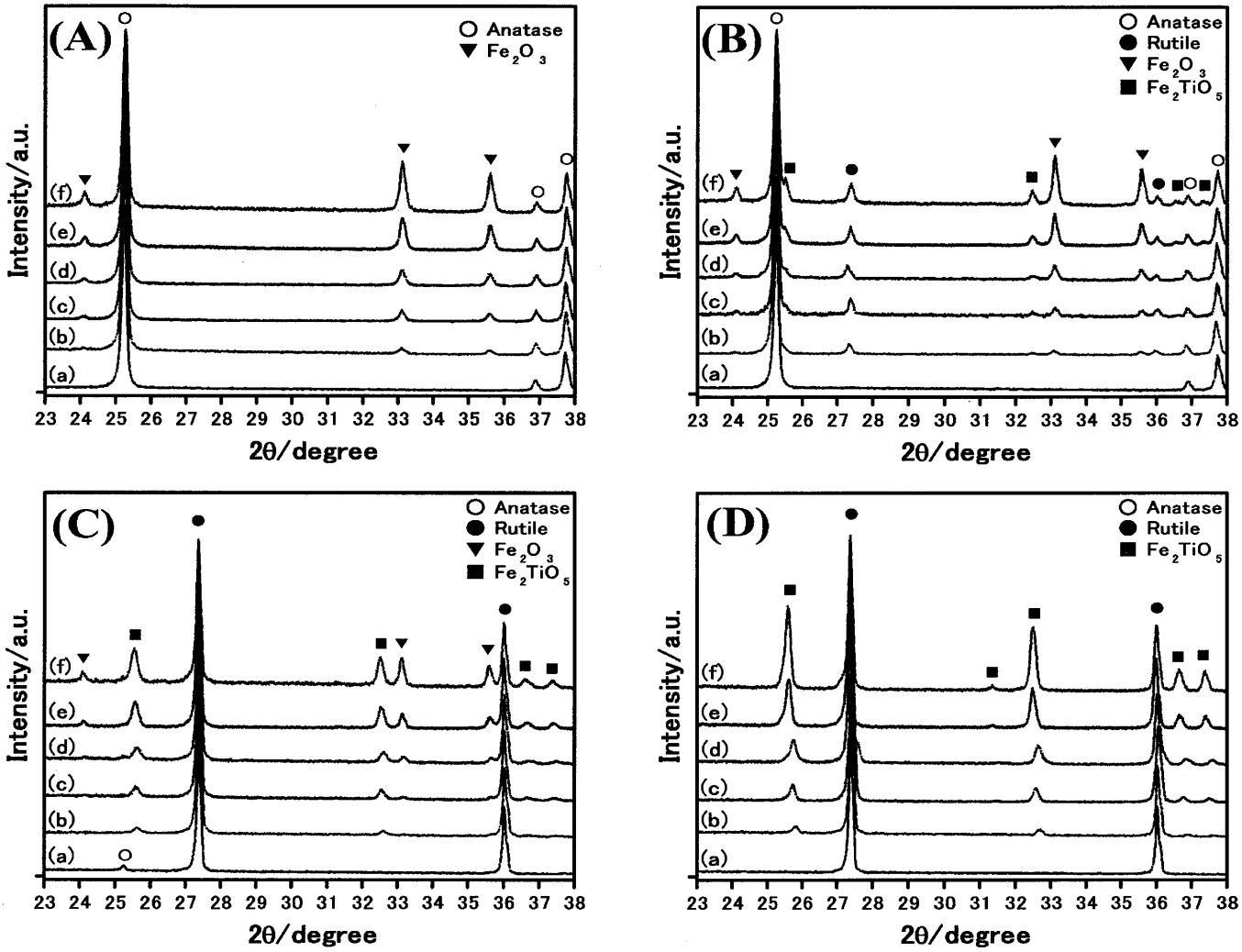

Fig.2 X-ray diffraction patterns of heat treated TiO_2 and TiO_2-Fe_3O_4 feedstock powders at various temperatures. (A) 973K, (B) 1123K, (C) 1273K, (D) 1423K. (Notes: (a) TiO_2 powder, (b) TiO_2-5wt.%Fe_3O_4 powder, (c) TiO_2-10wt.%Fe_3O_4 powder, (d) TiO_2-12.7wt.%Fe_3O_4 powder, (e) TiO_2-22.5wt.%Fe_3O_4 powder, (f) TiO_2-32.6wt.%Fe_3O_4 powder.)

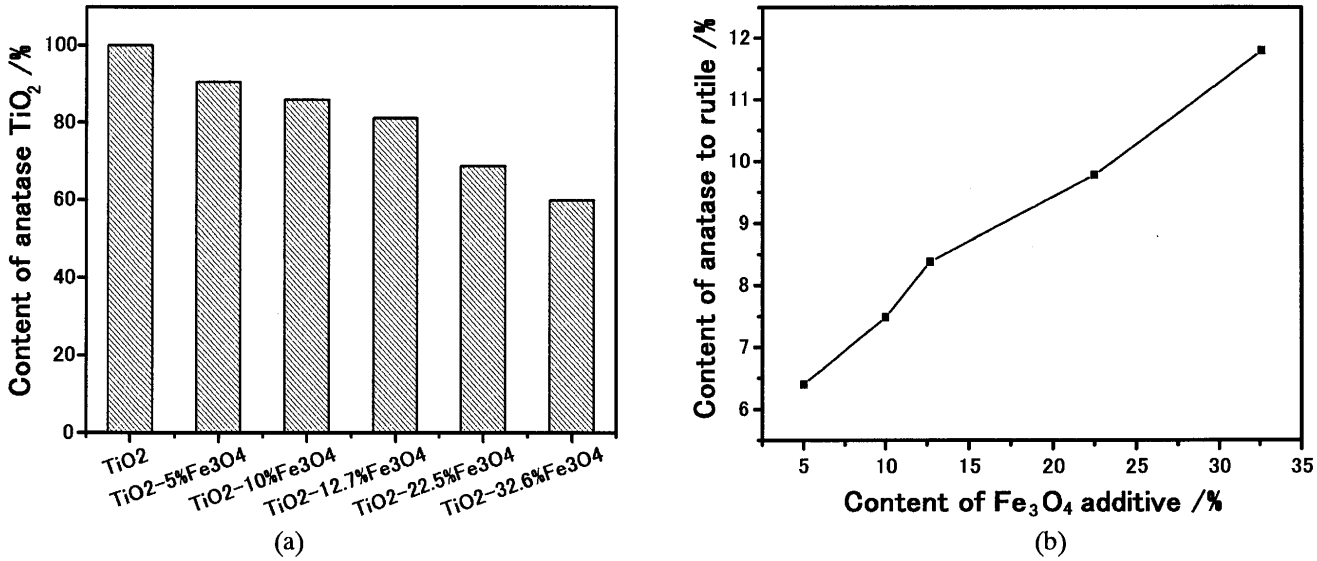

Fig.3 Content of anatase TiO_2 (a) and content of anatase TiO_2 transformed to rutile (b) in TiO_2 and TiO_2-Fe_3O_4 powders heat treated at 1123K.

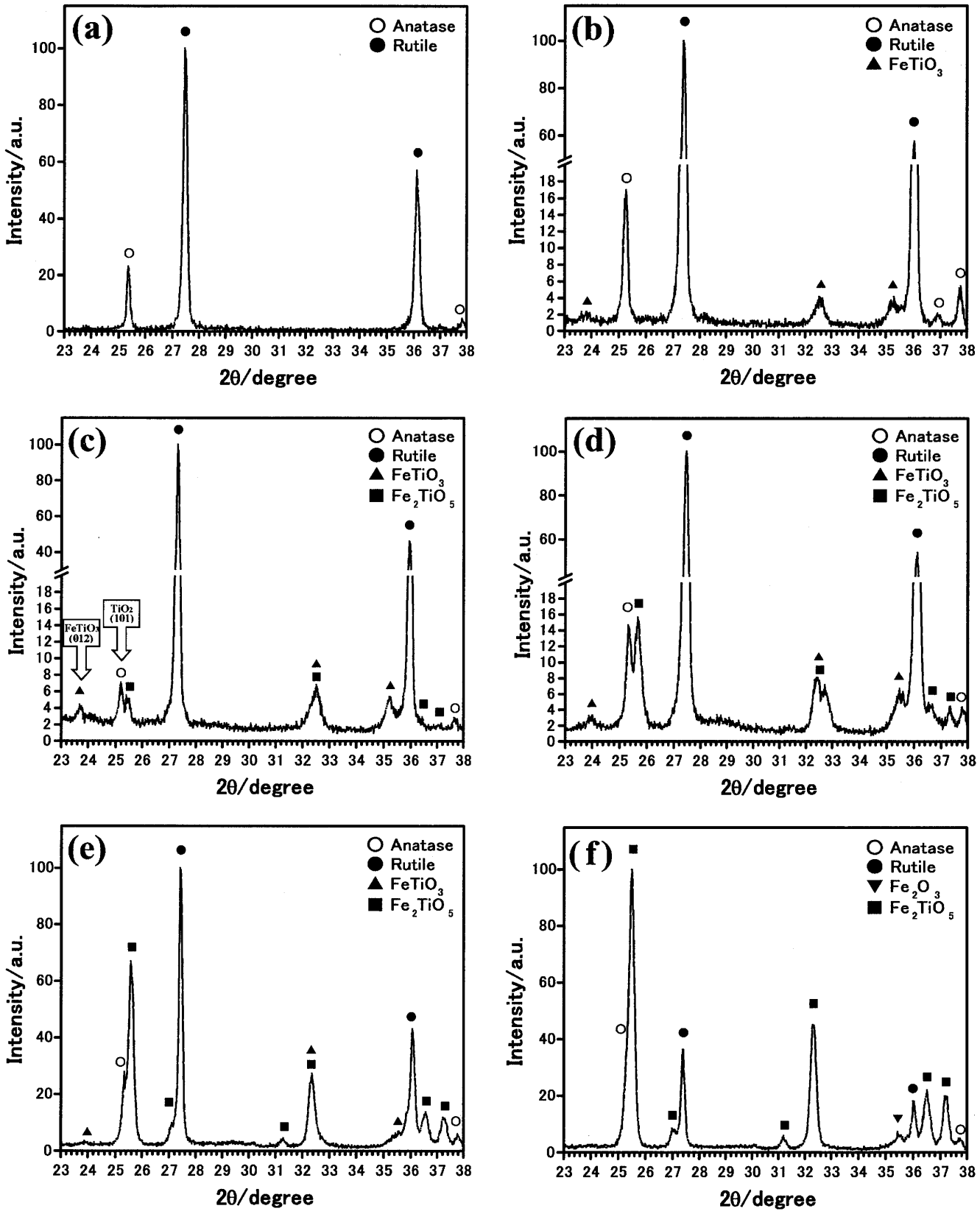

Fig.4 X-ray diffraction patterns of TiO_2 and TiO_2-Fe_3O_4 coatings plasma sprayed under the arc current of 400A and spraying distance of 70mm. (a) TiO_2 coating, (b) TiO_2-5wt.%Fe_3O_4 coating, (c) TiO_2-10wt.%Fe_3O_4 coating, (d) TiO_2-12.7wt.%Fe_3O_4 coating, (e) TiO_2-22.5wt.%Fe_3O_4 coating, (f) TiO_2- 32.6wt.%Fe_3O_4 coating.

It has been reported that because TiO_2 contains interstitial channels in the *c* direction, certain transition metals diffuse through these channels into lattices. The diffusing ions have been found to locate preferentially on either the substitutional or interstitial sites. Therefore, the formation of $FeTiO_3$ is possible in spite of the large ion radius of Fe^{2+}(0.83 Å)[26] especially in plasma spraying process for the instantaneous melting and solidification of the feedstock particles.

Furthermore, the formation of Fe_2TiO_5 is reported by the fact that certain percentage of Fe^{3+} ion diffuses into TiO_2 producing a substitutional solid solution where Fe^{3+} is dispersed in the lattice of TiO_2 due to the ion radius similarity of Fe^{3+}(0.67Å) and Ti^{4+}(0.64Å). The substitution of Fe^{3+} in the matrix of TiO_2 is a favorable process and is easier in rutile for the open channel[27]. This reason may result in the high amount of Fe_2TiO_5 in the sprayed coatings when more anatase TiO_2 particles transformed into rutile.

During the short residence time in the plasma jet, the feed particles are completely/partially melted. The droplets impact on a substrate and experience a cooling rate of 10^4~10^6K/s, therefore, the preferred orientation (PO) and amorphous body are exist widely[19), 20)]. These phenomena were found in the prepared TiO_2-Fe_3O_4 coating as clearly shown in **Fig.5**. The intensity of the main diffraction of rutile phase (110) increased slightly when the coating was crushed into micro-particles, which implied that PO existed in it. When the crushed coating was heat treated at 1273K for 2hr., the intensity of the main diffraction of rutile phase became higher than that of Fe_2TiO_5 phase. Therefore, amorphous bodies existed in the coating. These phenomena may make the quantitative analysis of the coatings using the abnormal intensities absolutely meaningless. As a result, great attentions should be paid on the quantitative measurement using the XRD method for thermal sprayed coating.

3.3 Energy absorbance of feedstock powders and sprayed coatings

The photocatalytic performance is affected by catalyst substance, light absorptive ability, morphology, and surface active site and so on. Because the light absorptive ability of the photocatalyst is a main factor to affect the photocatalytic activity, the diffuse reflectance of feedstock powders, sprayed TiO_2 and TiO_2-Fe_3O_4 coatings was investigated using the Shimadzu UV-3100PC scanning spectrophotometer. Generally, the photocatalytic activity increases with the increasing of light absorptive capacity[21)].

According to the diffuse reflectance spectra of the feedstock powders (**Fig.6**), the Fe_3O_4 additive did not change the absorption edge (wavelength coordinate of black circle in Fig.6) and the light absorbance drops suddenly in the wavelength range of 340nm to 400nm. The diffuse reflectance spectra of the sprayed coatings are shown in **Fig.7**, and to investigate the absorptive relation between light source used in this study and the sprayed coating, the spectral power distribution for UV-lamp is also illustrated in it. The light absorbance of the TiO_2 coating drop suddenly in the wavelength range of 340nm to 400nm. However, the dropping speed decreases continuously and the optical absorption edge (black circle) shifts to longer wavelength with the content increase of Fe_3O_4 additive. To compare the light absorptive capacity, the integrated energy absorbance of the sprayed TiO_2 and TiO_2-Fe_3O_4 coatings from the ultraviolet lamp used in this study was estimated according to equation (7). As shown in **Fig.8**, the relative integrated energy absorbance increases with the content increase of the Fe_3O_4 additive, which means that more irradiation light energy can be utilized. It partly ascribe to $FeTiO_3$ and Fe_2TiO_5 compound as reported by B. Pal et al.[27], N. Smirnova et al.[28], and F. X. Ye et al.[11].

3.4 Photocatalytic activity of plasma sprayed TiO_2 and TiO_2-Fe_3O_4 coatings

Fig.9(a) illustrates the decomposition characteristic of the acetaldehyde by the sprayed TiO_2 and TiO_2-Fe_3O_4 coatings. It indicates that the plasma sprayed coatings can decompose acetaldehyde under illumination by ultraviolet rays and the photocatalytic activity of TiO_2-10wt.%Fe_3O_4 coating was better than that of the other coatings. According to the equation (8), the τ values of the sprayed TiO_2 and TiO_2-Fe_3O_4 coatings were calculated as shown in **Fig.9(b)**. The photocatalytic activity increases with the increasing of Fe_3O_4 weight to 10% firstly, but then decreases. As discussed in coating composition section, the amount of $FeTiO_3$ phase in the sprayed TiO_2-10wt.%Fe_3O_4 coating is highest, and the content of Fe_2TiO_5 phase increased substantially when the amount of Fe_3O_4 additive is over 10%.

The good photocatalytic efficiency of TiO_2-10wt.%Fe_3O_4 coating possibly results from the high content of ilmenite $FeTiO_3$ phase in the coating, because $FeTiO_3$ (band gap: 2.58eV) has good light absorbance and favorable photo-excited electron-hole separation characters[11]. The band gap of pure Fe_2TiO_5 is 2.18eV, which is much lower than that of TiO_2 and $FeTiO_3$. Although the light absorbance increases with the amount increasing of Fe_2TiO_5 compound, the photocatalytic activity is reduced dramatically when the content of Fe_2TiO_5 is high. As is known[27], this kind of phenomenon may result from the unfavorable charge transfer process to adsorbed substance during light illumination where excess accumulation of electron and hole undergoes recombination immediately without taking part in the photocatalytic reaction. Therefore, the electron-hole pair formation and separation process is a key factor in photocatalytic reaction.

As a result, the photocatalytic efficiency of sprayed TiO_2-Fe_3O_4 coating is improved with an increase of $FeTiO_3$ content. However, when the content of Fe_3O_4

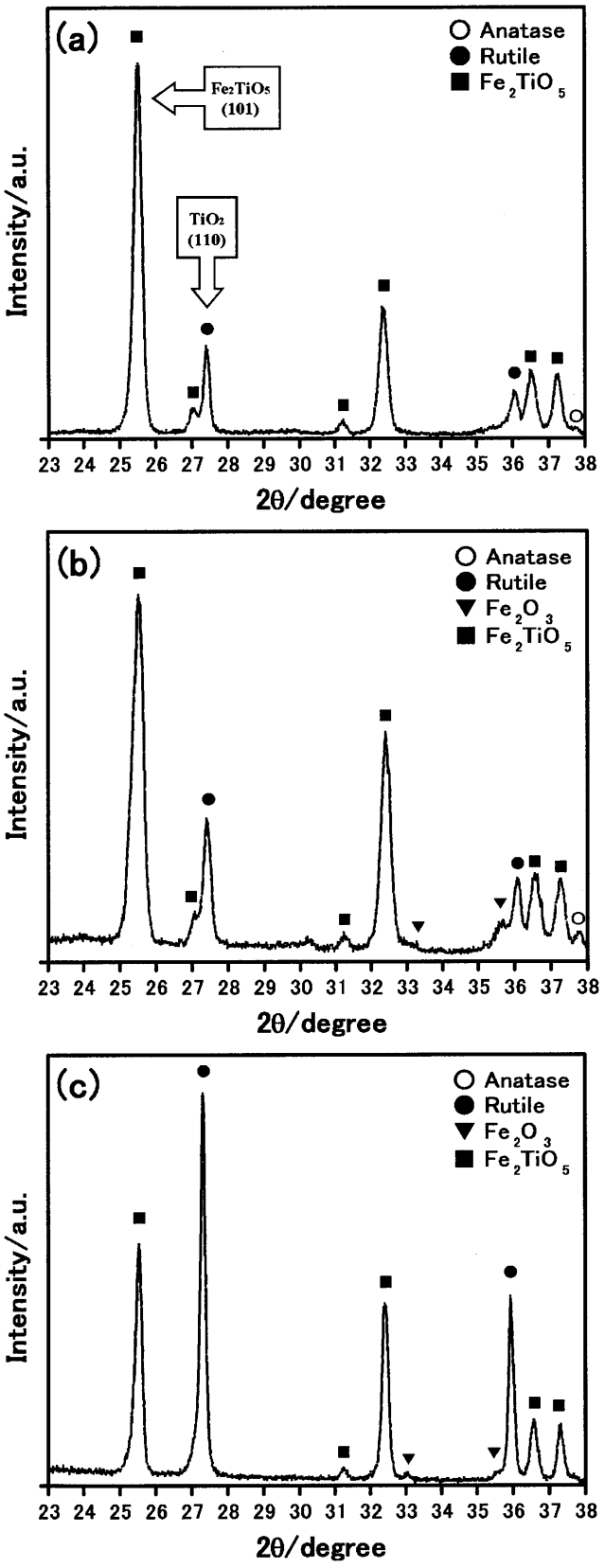

Fig.5 Phase changes after various processes of TiO_2-32.6%Fe_3O_4 coating prepared under the arc current of 600A. (a) original coating, (b) crushed coating, (c) heat treated at 1273K of (b).

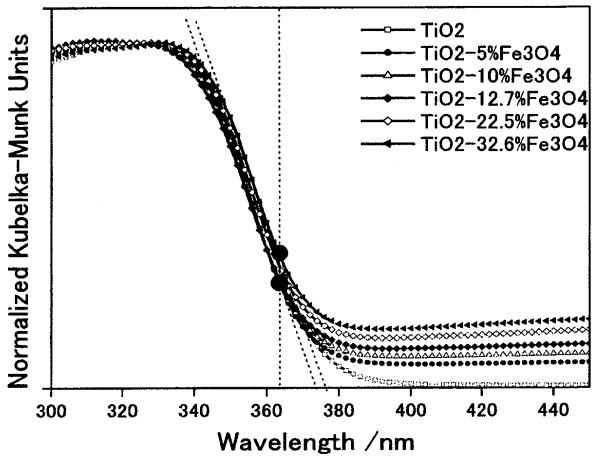

Fig.6 The diffuse reflectance spectra of the feedstock TiO_2 and TiO_2-Fe_3O_4 powders.

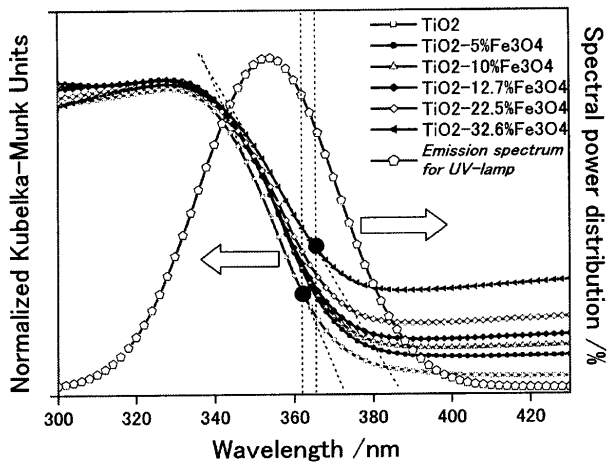

Fig.7 The diffuse reflectance spectra of the sprayed TiO_2, TiO_2-Fe_3O_4 coatings and the spectral power distribution for the ultraviolet lamp used in this study.

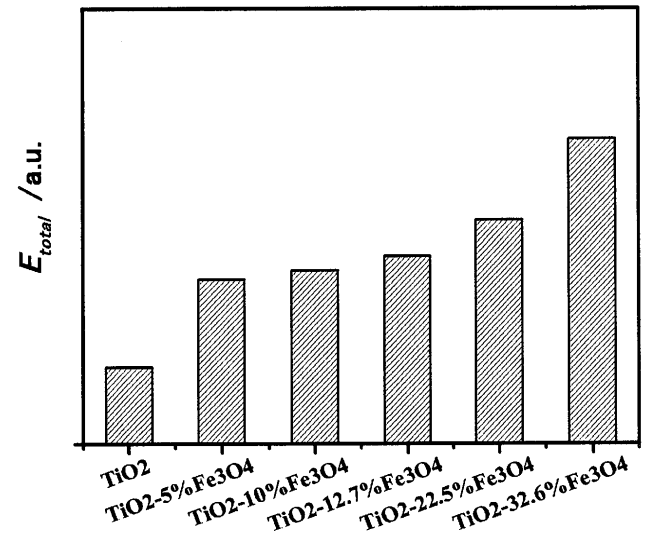

Fig.8 The integrated energy absorbance of the sprayed TiO_2 and TiO_2-Fe_3O_4 coatings from the ultraviolet lamp used in this study.

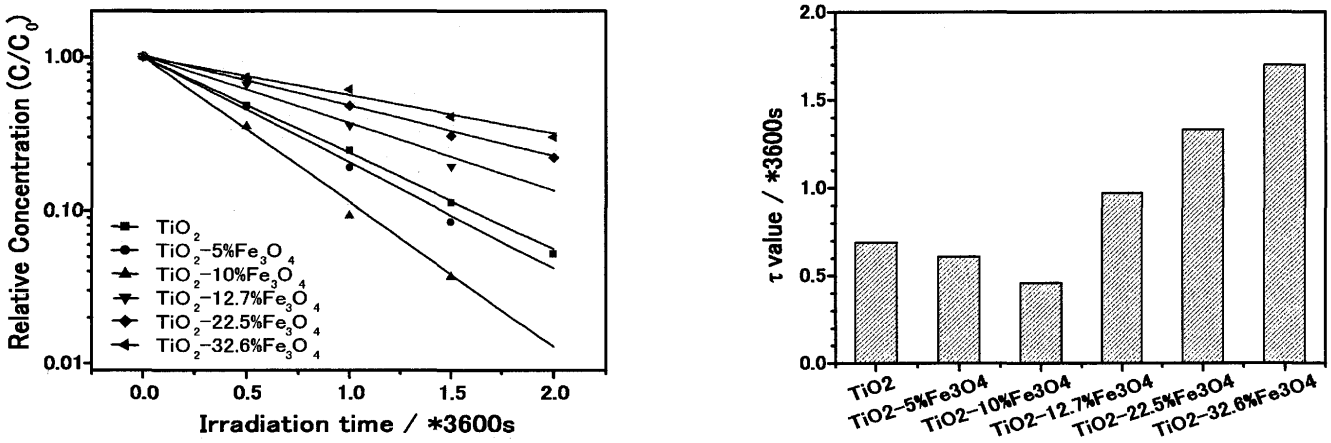

(a) (b)

Fig.9 Photocatalytic decomposition characteristics (a) and τ values (b) of the sprayed TiO_2 and TiO_2-Fe_3O_4 coatings.

additive is over 12.7%, photocatalytic activity is reduced to large extent due to the presence of large amount of inactive Fe_2TiO_5 compound in the TiO_2-Fe_3O_4 coatings.

4. Conclusions

TiO_2 and TiO_2-Fe_3O_4 coatings were prepared on stainless steel substrate by plasma spraying. The results clearly showed that the TiO_2-Fe_3O_4 coatings consist of anatase TiO_2, rutile TiO_2, and pseudobrookite Fe_2TiO_5 phase which appeared when the content of Fe_3O_4 additive is equal to or over 10%. With relative low amount addition of Fe_3O_4, ilmenite $FeTiO_3$ phase exists in the sprayed coatings. The content of anatase TiO_2 in the sprayed coatings decreases with the increasing of Fe_3O_4 content. The addition of Fe_3O_4 improved anatase-rutile transformation. It was observed that TiO_2 coatings deposited on stainless steel have the photocatalytic activity, and the degrading efficiency of acetaldehyde is improved with an increase of $FeTiO_3$ content in the coatings. However, presence of large amount of Fe_2TiO_5 compound substantially reduces the photocatalytic efficiency of the sprayed TiO_2-Fe_3O_4 coatings for its unfavorable electron-hole transfer process.

References

1) A. Fujishima, K. Honda, Nature 238 (1972) 37.
2) A. Fujishima, T.N. Rao, D.A. Tryk, J. Photoch. Photobio. C: Photoch. Rev. 1 (2000) 1.
3) J.A. Navio, G. Colon, et.al., J. Mol. Catal. A-Chem. 109 (1996) 239.
4) J.A. Navio, G. Colon, J.M. Herrmann, J. Photoch. Photobio. A 108 (1997) 179.
5) L. Bahadur, N.R. Tata, J. Photoch. Photobio. A 91 (1995) 233.
6) M.R. Dhananjeyan, V. Kandavelu, R. Renganathan, J. Mol. Catal. A-Chem. 151 (2000) 217.
7) Pal, T. Hata, K. Goto, G. Nogami, J. Mol. Catal. A-Chem. 169 (2001) 147.
8) A.K.G. Carlos, F. Wypych, S.G. Moraes, N. Duran, N. Nagata, P. Peralta-Zamora, Chemosphere 40 (2000) 433.
9) B. Neppolian, H. C. Choi, S. Sakthivel, Banumathi Arabindoo and V. Murugesan, J. Harz. Mater. 89 (2002) 303.
10) L. Bayer, I. Eroglu, L. Turker, Sol. Energ. Mat. Sol. C. 62 (2000) 43.
11) F. X. Ye and A. Ohmori, Surf. Coat. Technol., 160 (2002) 62.
12) P. Calza, C. Minero, A. Hiskia, Appl. Catal. B-Environ. 21 (3) (1999) 191.
13) A. Mills, J. Wang, J. Photoch. Photobio. A 127 (1999) 123.
14) K. Tennakone, U.S. Ketipearachchi, Appl. Catal. B-Environ. 5 (1995) 343.
15) F. Zhang, J. Zhao, T. Shen, H. Hidaka, E. Pelizzetti, N. Serpone, Appl. Catal. B-Environ. 15 (1998) 147.
16) A. Sclafani, J. Herrmann, J. Photoch. Photobio. A 113 (2) (1998) 181.
17) Ilisz, Z. Laszlo, A. Dombi, Appl. Catal. A-Gen. 180 (1999) 25.
18) B. D. Cullity, Elements of x-ray diffraction, Second edition, 1978 P397-419.
19) P. Bansal, N. P. Padture, A. Vasiliev, Acta Materialia, 51 (2003) 2959.
20) Y. Z. Yang, Z. G. Liu, Z. Y. Liu, Y. Z. Chuang, Thin Solid Films, 388 (2001) 208.
21) Z. Zou, J. Ye, K. Sayama, H. Arakawa, Chem. Phys. Lett. 343 (2001) 303.
22) P. D. Fochs, Proc. Phys. Soc., B69 (1956) 70
23) S. P. Tandon, J. P. Gupta, Phys. Stat. Sol. 38 (1970) 363.
24) A.V. Vorontsov, A.A. Altynnikov, J. Photochem. Photobiol. A 144 (2001) 193.
25) P.H. Chen, C.H. Jenq, Environ. Int. 24 (8) (1998) 871.
26) K. H. Yoon, J. Cho and D. H. Kang, Mater Res. Bull. 34, No. 9 (1999) 1451.
27) B. Pal, M. Sharon and G. Nogami, Mater. Chem. Phys. 59 (1999) 254.
28) N. Smirnova, A. Eremenko, O. Rusina, W. Hopp, L. Spanhel, J. Sol-gel Sci. Tech. 22 (1-2) (2001) 109.